Published December 16, 2013

Protonation controls ASIC1a activity via coordinated movements in multiple domains

Gaetano Bonifacio, Cláudia Igutti Suenaga Lelli, and Stephan Kellenberger

Department of Pharmacology and Toxicology, University of Lausanne, 1005 Lausanne, Switzerland

Acid-sensing ion channels (ASICs) are neuronal Na^+-conducting channels activated by extracellular acidification. ASICs are involved in pain sensation, expression of fear, and neurodegeneration after ischemic stroke. Functional ASICs are composed of three identical or homologous subunits, whose extracellular part has a handlike structure. Currently, it is unclear how protonation of residues in extracellular domains controls ASIC activity. Knowledge of these mechanisms would allow a rational development of drugs acting on ASICs. Protonation may induce conformational changes that control the position of the channel gate. We used voltage-clamp fluorometry with fluorophores attached to residues in different domains of ASIC1a to detect conformational changes. Comparison of the timing of fluorescence and current signals identified residues involved in movements that preceded desensitization and may therefore be associated with channel opening or early steps leading to desensitization. Other residues participated in movements intimately linked to desensitization and recovery from desensitization. Fluorescence signals of all mutants were detected at more alkaline pH than ionic currents. Their midpoint of pH dependence was close to that of steady-state desensitization, whereas the steepness of the pH fluorescence relationship was closer to that of current activation. A sequence of movements was observed upon acidification, and its backward movements during recovery from desensitization occurred in the reverse order, indicating that the individual steps are interdependent. Furthermore, the fluorescence signal of some labeled residues in the finger domain was strongly quenched by a Trp residue in the neighboring β-ball domain. Upon channel activation, their fluorescence intensity increased, indicating that the finger moved away from the β ball. This extensive analysis of activity-dependent conformational changes in ASICs sheds new light on the mechanisms by which protonation controls ASIC activity.

INTRODUCTION

This study investigates the conformational changes of an acid-sensing ion channel (ASIC) during different functional transitions to obtain information on how protonation of extracellular amino acid residues activates these channels. ASICs are proton-gated Na^+ channels of the nervous system that are involved in pain sensation, the expression of fear, and neurodegeneration after ischemic stroke (Xiong et al., 2004; Sluka et al., 2009; Ziemann et al., 2009). They are formed by trimers of identical or homologous subunits (Jasti et al., 2007; Gonzales et al., 2009; Dawson et al., 2012). Each subunit contains intracellular amino and carboxy termini and two transmembrane segments connected by a large extracellular loop. The channel structure has been compared with three hands arranged back to back around the central ion pore (Fig. 1 A) (Jasti et al., 2007). The finger domains are located at the upper, external edge of the protein, slightly higher than the knuckle and the β ball (Fig. 1, A and B). The finger, β ball, and thumb enclose together in each subunit the "acidic pocket," which contains a network of acidic residues involved in pH sensing (Fig. 1, A and C) (Jasti et al., 2007). The palm domains are arranged along the central vertical axis of the trimer and form the covalent link between the extracellular domains and the transmembrane segments, which contain the channel gates (Fig. 1, A and D) (Li et al., 2011; Baconguis and Gouaux, 2012). An additional, noncovalent link between the extracellular and transmembrane parts is provided by the β turn, located in a loop between the thumb and the palm, pointing to the upper end of the first transmembrane segment (Li et al., 2009).

ASICs open upon extracellular acidification and desensitize within hundreds of milliseconds. Desensitized ASICs do not conduct any current and can be activated again only after exposure to a sufficiently alkaline pH. The ASIC gating can be described with a kinetic model that contains after protonation a closed, an open, and a desensitized state (Fig. 1 E) (Li et al., 2012). There is evidence that protonation of several residues per subunit, located in different extracellular domains, is required

Correspondence to Stephan Kellenberger: Stephan.Kellenberger@unil.ch

Abbreviations used in this paper: ASIC, acid-sensing ion channel; ENaC, epithelial Na^+ channel; SSD, steady-state desensitization; VCF, voltage-clamp fluorometry.

The Rockefeller University Press $30.00
J. Gen. Physiol. Vol. 143 No. 1 105–118
www.jgp.org/cgi/doi/10.1085/jgp.201311053

Supplemental Material can be found at:
http://jgp.rupress.org/content/suppl/2013/12/15/jgp.201311053.DC1.html

Published December 16, 2013

for normal activation and desensitization of ASICs (Paukert et al., 2008; Liechti et al., 2010). We hypothesize that protonation of proton-sensing residues induces conformational changes that are transmitted to the channel gate. Knowledge of conformational changes involved in the different ASIC gating transitions would allow us to understand the molecular mechanisms by which pH controls ASIC activity. The published crystal structures, corresponding likely to the open and desensitized states, indicate that differences between these two states exist mainly in the pore and palm domains (Jasti et al., 2007; Gonzales et al., 2009; Baconguis and Gouaux, 2012; Dawson et al., 2012). The conformation of the closed channel is not known. To understand the ASIC gating mechanisms, it would be important to know the conformational changes occurring when the channel opens or desensitizes from the closed state. One study applied voltage-clamp fluorometry (VCF) to show that a Glu residue located in the extracellular pore entrance undergoes rapid conformational changes (Passero et al., 2009). However, this study did not analyze other residues. Therefore, it is currently not known which conformational changes the ASICs have to undergo to reach the open state or to desensitize. The aim of the present study was to identify residues of different extracellular domains involved in conformational changes, and to determine to which gating transitions the reported conformational changes are associated. To this end, we placed environment-sensitive fluorophores at specific sites in different extracellular domains of ASIC1a and used VCF (Mannuzzu et al., 1996; Cha and Bezanilla, 1997). Comparison of the timing of fluorescence and current signals measured by VCF allows association of conformational changes with channel function. VCF has a higher temporal resolution than indirect functional approaches such as state-dependent chemical modification of engineered Cys residues. This study identifies residues of ASIC1a that are involved in conformational changes and associates some of them with specific gating transitions. It also shows that the finger moves away from the β ball upon channel activation.

MATERIALS AND METHODS

Molecular biology

Human ASIC1a was subcloned into a pSP65-derived vector containing 5′ and 3′ nontranslated sequences of *Xenopus laevis* β-globin, which allows a higher expression in *Xenopus* oocytes. Site-directed mutagenesis was performed using QuikChange (Agilent Technologies). Mutations were verified by sequencing (Synergene Biotech). In vitro transcription was performed using the mMESSAGE mMACHINE SP6 kit (Ambion/Applied Biosystems).

Oocyte handling and injection

All experimental procedures on *Xenopus* were performed in accordance with the Swiss federal law on animal welfare and had been approved by the committee on animal experimentation of the Canton de Vaud. Healthy stage V and VI oocytes from female *Xenopus* were treated by collagenase and de-folliculated, isolated, and subsequently injected with 50 nl cRNA (0.5 µg/µl). 2 h after RNA injection, oocytes were incubated in 10 mM 3-maleimidopropionic acid (Bachem) dissolved in Modified Barth's solution (MBS) for 1 h to modify the free Cys residues of proteins natively present on the membrane surface, and were then kept in MBS composed of (mM) 85 NaCl, 1 KCl, 2.4 $NaHCO_3$, 0.33 $Ca(NO_3)_2$, 0.82 $MgSO_4$, 0.41 $CaCl_2$, 10 HEPES, and 4.08 NaOH for 36–48 h. Expression and current measurements with the epithelial Na^+ channel (ENaC) were done as described previously (Kellenberger et al., 1999).

Solutions and reagents

Recording solutions contained (mM) 110 NaCl, 2 $CaCl_2$, and 10 HEPES for pH values >6.8. In solutions with a pH of ≤6.8, HEPES was replaced by 10 mM Mes. The pH of all the above-mentioned solutions was adjusted using NaOH. 10-mM stock solutions of Alexa Fluor 488 C-5 Maleimide (AF488; Invitrogen) and CF 488A (Biotium) were prepared in DMSO; aliquots were stored at −20°C.

VCF

All experiments were performed with fluorophore-labeled channels. Oocytes were labeled in the dark by 5 µM Alexa Fluor 488 C-5 maleimide (AF488; Invitrogen) or CF 488A maleimide (Biotium), as indicated in Table S1, for 20–30 min at 19°C. Lifetimes of the excited states of such fluorophores are of the order of nanoseconds; therefore, they are well suited to follow rapid conformational changes in ion channels (Cha and Bezanilla, 1998). Oocytes were placed in an RC-25 recording chamber (Warner Instruments), impaled with two glass microelectrodes filled with 1 M KCl with a resistance of <0.4 MΩ, and perfused by gravity at a rate of 12 ml/min. Currents were recorded with an amplifier (TEV-200A; Dagan Corporation) at −40 mV using pClamp software (Molecular Devices).

The VCF setup was constructed similar to previously reported setups (Meinild et al., 2002; Virkki et al., 2006). It was equipped with an Intensilight lamp (C-HGFI; Nikon). A 40× oil-immersion objective (CFI Plan Fluor; Nikon) was used to detect the signal emitted by the labeled oocyte. The optical unit containing objective and filter cube (excitation, 480 ± 20 nm; emission, 535 ± 25 nm; dichroic mirror, 510 nm; Chroma Technology Corp.) was mounted on an X–Y translation stage (M406; Newport) to allow fine movements of the objective under the perfusion chamber. An electronic shutter (VS252T1; Uniblitz; Vincent Associates) was mounted between the filter cube entrance and the light source. Its opening was controlled via the 1322A interface (Molecular Devices). The fluorescence signal was measured by a photodiode (S1336-18BQ; Hamamatsu Photonics) mounted on the headstage of an amplifier (List EPC-7; HEKA). A scalable offset device was used to adjust and measure the offset of the signal, allowing the measurement of the total fluorescence intensity F. Changes in fluorescence intensity (ΔF) were normalized to the total fluorescence intensity as ΔF/F. The signal was filtered and amplified by a low-pass eight-pole Bessel filter (LPF-8; Warner Instruments) at 40 Hz.

Kinetics of solution change

In the experiments reported here, the fluorescence signal was measured from a limited region of the oocyte vegetal pole that was oriented toward the solution inlet. Its surface had a diameter of ∼0.5 mm and corresponded to ∼20% of the total oocyte surface. The current signal was measured from the entire oocyte surface. We expressed the constitutively active ENaC and changed the extracellular recording solution from one containing K^+ to the normal solution containing Na^+ to monitor the kinetics of solution change as the appearance of ENaC current. Because in these experiments the K^+ solution had a pH of 7.4 whereas the Na^+ solution had the pH adjusted to 6, we were able to monitor the solution change in the area of fluorescence measurement by the pH-dependent plasma membrane resident fluorophore *N*-(fluorescein-5-thiocarbonyl)-1,

Published December 16, 2013

2-dihexadecyl-sn-glycero-3-phosphoethanolamine (Biotium; Fig. S1, A and B). We observed a delay that is caused by the dead volume in the tube after the junction where the different tubes come together. This delay was 685 ± 27 ms for the ΔF and 597 ± 24 ms for the current signal (n = 14), indicating a delay of <100 ms between the two types of signals (Fig. S1 C). The rise time of solution change, determined as the time necessary to pass from 10 to 90% of the maximal amplitude, was 346 ± 13 ms as measured by the fluorescence change and 301 ± 19 ms as measured by the Na^+ current appearance (n = 14; Fig. S1 D). This indicates that the kinetics of solution change are very similar and only slightly slower at the oocyte surface used for measuring the fluorescence signal, but that they are not fast enough to resolve processes with rise times faster than ∼300 ms. In WT ASIC1a and the tested mutants, the rise time of current appearance was 100–300 ms (see Results). This indicated that the observed current appearance with ASIC1a is faster than solution change, suggesting that some of the channels open before pH 6.0 is reached in their proximity. To test the reproducibility of the kinetics of solution change between different experimental days, we compared for the three mutants K133C, E355C, and E427C the kinetics recorded at different dates that were for each mutant several months apart. The average rise time difference between the two dates was for these mutants: 36, 162, and 97 ms for the current, and 101, 179, and 58 ms for the fluorescence signal (n = 3–8 per mutant and date). This indicates that the kinetic data are reproducible within the limits of approximately ±200 ms. The current and ΔF kinetics of rapid transitions (opening and desensitization) were compared in the same experiments. The change in the average ΔF/current rise time ratio between two experimental dates was within ±12, ±20, and ±15% in the three mutants K133C, E355C, and E427C.

Collectively, these controls indicate first that the solution change for ΔF and the current signals had very similar kinetics. Second, they set the following limits for the resolution and reproducibility of current and ΔF kinetics: The solution change occurs with a rise time of ∼300 ms, and measured rise times are reproducible within the error limits of approximately ±200 ms; the ΔF/current rise time ratio is reproducible within ±20%.

Data analysis

Both current and fluorescence signals were recorded by Clampex 9.2 software (Molecular Devices) at a sampling rate of 10 kHz. The pH of half-maximal activation (pH_{50}) was determined by fitting normalized activation curves to the Hill equation ($I = I_{max}/(1 + (10^{-pH50}/10^{-pH})^{nH})$), where I_{max} is the maximal current, pH_{50} is the value at which the current amplitude is half-maximal, and nH is the Hill coefficient (Kaleidagraph 4.0; Synergy Software). The pH of half-maximal steady-state desensitization (SSD) was determined by fitting the experimental data to an analogous Hill equation. Analysis of amplitude and rise time was performed using Clampfit 9.2 software (Molecular Devices). Kinetics of SSD and recovery were fitted by using a single-exponential equation, except for the $\tau F_{recovery}$ of mutant E427C that was fitted using a double exponential. ΔF, current onset, and decay kinetics in the context of channel activation were determined as rise (or decay) time. Images of cASIC1 molecular structure were obtained by using UCSF Chimera software v1.6.2 (Pettersen et al., 2004). Current and ΔF kinetics were considered as similar if they were not statistically different (ANOVA followed by Tukey post-hoc test; $P > 0.05$) and if their ratio was between 1.4 and 0.71. All data shown are expressed as mean ± SEM of independent experiments.

Online supplemental material

Table S1 provides estimates of the upper limit of possible contributions of an intrinsic pH dependence of the fluorophores to the ΔF signal. Fig. S1 shows an analysis of the solution exchange kinetics on the cellular surfaces used for the current and fluorescence measurements. Fig. S2 shows two examples of mutants that did not produce a measurable ΔF signal. Fig. S3 presents the kinetics of the ΔF onset and of the current decay at several pH values for the mutants associated with desensitization. Fig. S4 indicates the pH of half-maximal amplitude and Hill coefficients of ΔF and current activation and SSD of all analyzed mutants, derived from experiments illustrated in Fig. 5. Fig. S5 addresses the pH dependence of recovery from desensitization and shows that the kinetics of ΔF and current recovery do not depend on the stimulation pH but are a function of the conditioning pH to which the channels are exposed after the acidic stimulation. Fig. S6 presents an analysis of quenching by iodide of ΔF of selected mutants. Fig. S7 shows representative current and ΔF traces of double mutants containing an engineered Cys residue that after labeling had produced a ΔF, together with the mutation of the endogenous residue Trp 233 to Val. The online supplemental material is available at http://www.jgp.org/cgi/content/full/jgp.201311053/DC1.

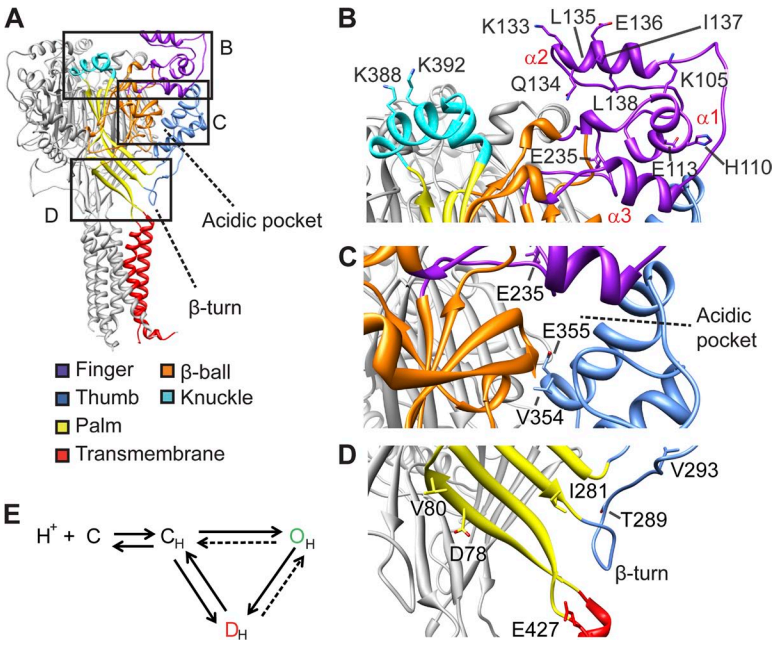

Figure 1. Fluorophores placed at distinct sites of the ASIC protein report conformational changes. (A) Structural model of ASIC1a, based on the crystal structure of chicken ASIC1 (Jasti et al., 2007), with the domains in one subunit indicated by differential coloring. The frames indicate part of the structure shown in close-up view in B–D. (B–D) Detailed views indicating the localization of the residues that were mutated to Cys for labeling by fluorophores. (B) Finger and knuckle domains, (C) Acidic pocket, (D) palm and palm-thumb loop with β turn. (E) ASIC gating scheme. Protonation (C_H) leads to a transient opening (O_H) followed by channel desensitization (D_H) or, upon mild acidification, to desensitization from the closed state (SSD).

Published December 16, 2013

RESULTS

Fluorophores placed in different extracellular domains report environmental changes during ASIC activity

ASIC1a mutants containing an engineered Cys residue were expressed in *Xenopus* oocytes and labeled on the introduced Cys residue by a thiol-reactive, intrinsically pH-independent and membrane-impermeant fluorophore (Alexa Fluor 488; Invitrogen; or CF488; Biotium). Ionic currents and changes in fluorescence (ΔF) were simultaneously measured in response to extracellular pH changes from the conditioning pH 7.4 to several acidic stimulation pH values. Fluorophore positions in all extracellular domains were tested. Out of 75 functional mutants that each contained an engineered Cys residue at a position that was estimated to be solvent accessible based on the crystal structures, 20 showed consistent ΔF signals (Fig. 1, A–D). Of the 55 mutants that did not produce ΔF signals after labeling (see examples in Fig. S2), 6 displayed low current amplitudes and were therefore

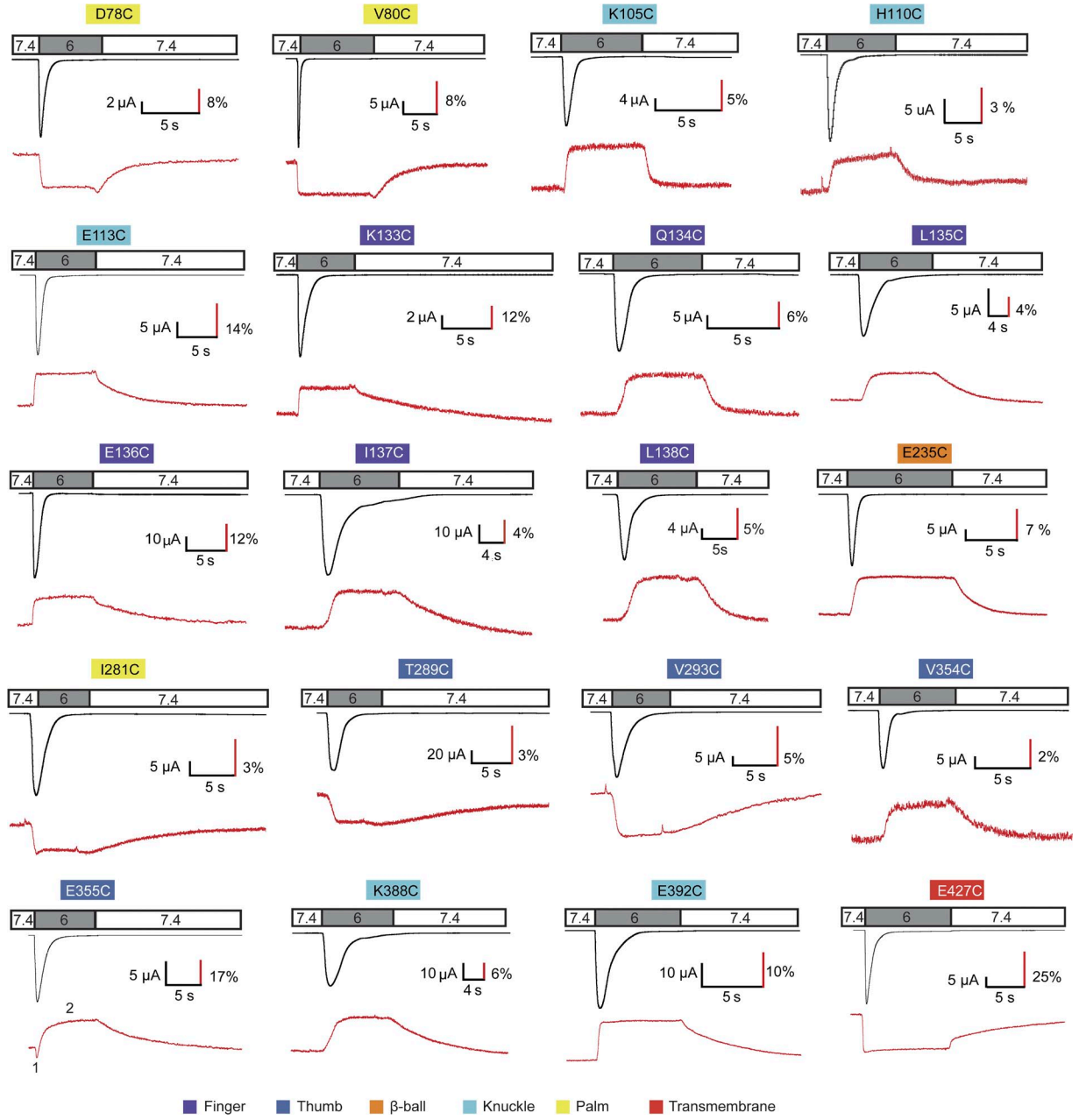

Figure 2. Representative current and ΔF traces. ASIC1a currents (black traces) and ΔF signals (red traces) were recorded simultaneously from oocytes under voltage clamp to −40 mV that expressed the indicated ASIC1a mutant in which the engineered Cys residue had been labeled by Alexa Fluor 488 or CF488 before recording. The timing of the extracellular solution changes is indicated in the bar above the traces. The small ΔF peaks of V293C and I281C represent artifacts caused by the solution change. The color shading of the labels indicates of which domains the mutants are part. The numbering in the E355C ΔF trace indicates the two components of the signal.

Published December 16, 2013

probably not expressed at sufficiently high level to generate a detectable ΔF signal. In many of the other mutants not producing a ΔF signal, the attached fluorophore likely underwent conformational changes but was not located close enough to quenching groups or did not sufficiently change its solvent exposure. All the 20 positive mutants showed the typical transient ASIC currents. Their current kinetics and pH dependence were similar to ASIC1a WT. The fluorescence signal, however, increased or decreased upon channel activation with kinetics that differed between mutants (Fig. 2). For example, in the mutants containing the engineered Cys residue in the finger domain, the fluorescence amplitude increased rapidly when the channels were exposed to an acidic pH, and the fluorescence intensity did not further change during the acidification. After switching back to the conditioning pH 7.4, the fluorescence returned to the baseline. In many mutants, these return kinetics were substantially slower than the kinetics of the ΔF onset. The mutant E355C showed first a rapid decrease in fluorescence, followed by a slower increase. E355 is located at the lower end of the α5 helix of the thumb, in close proximity to β-ball residues of a neighboring subunit (Fig. 1 C). The biphasic ΔF may represent conformational changes associated with two distinct transitions.

Specificity of the fluorescence signal

Mutants were generated in WT human ASIC1a because the only unpaired extracellular Cys residue, Cys 275, appeared not to be labeled by the fluorophore, and mutant C275A as well as WT ASIC1a did not produce measurable fluorescence changes (Fig. 3, A and B). The 20 mutants displaying a measurable ΔF described in this study represent 30% of the tested mutants. The absence of ΔF in the other ∼70% of tested mutants and in WT indicates that the ΔF measured in the positive mutants is a result of specific labeling of the engineered Cys residue.

The fluorescence of both Alexa Fluor 488 and CF488A is known to be pH independent over a wide range. To test for any intrinsic pH dependence of the fluorophore in our experimental setting, labeled channels were first exposed for 30 s to a conditioning pH that desensitized them (generally pH 6.9), followed by exposure to the stimulation pH 6. Under these conditions, pH 6.0 stimulation does not induce any currents (Fig. 3 C), and fluorescence changes associated with channel activity are not expected to occur. The presence of a ΔF in the closed-to-open (pH 7.4→pH 6; Fig. 3 D) but not in the desensitized-to-open protocol (pH 6.9→pH 6; Fig. 3 C) would prove the absence of ΔF contributions unrelated to known gating transitions, such as pH-dependent effects on the fluorophore itself or on its fluorescence signal by protonation of residues in its direct environment. In 18 out of the 20 mutants, the amplitude of the ΔF in the desensitized-to-open protocol amounted to <16% of the amplitude measured in the closed-to-open protocol. This shows that contamination of the measured fluorescence signals by ΔF caused by the intrinsic pH dependence of the fluorophores or by protonation of residues in its direct environment not participating in conformational changes makes up <16% of the recorded ΔF amplitude (Fig. 3, C and D, and Table S1). In the mutants E136C and T289C, the desensitized-to-open ΔF corresponded to 24 and 20% of the closed-to-open ΔF, respectively. For these two fluorophore positions, the charge of residues in the proximity of the fluorophore may affect its pKa and may thereby change the range of its pH independence. Alternatively, the ΔF measured in

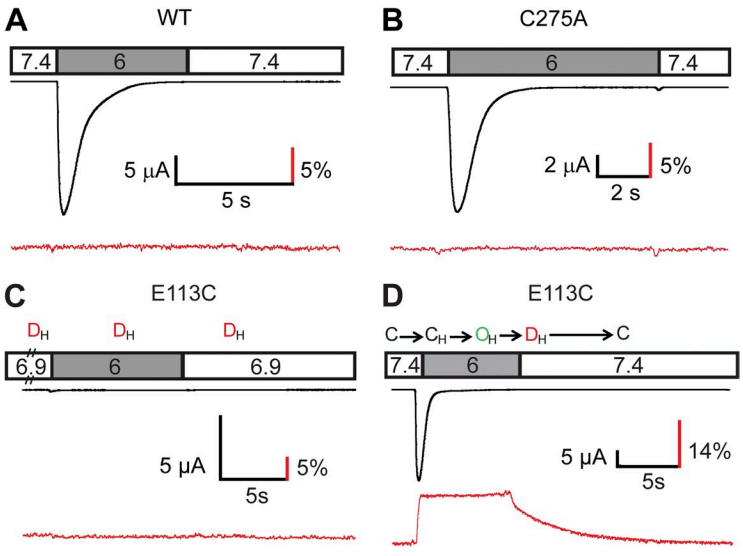

Figure 3. Control experiments for endogenous Cys residue of ASIC1a and intrinsic pH dependence of fluorophores. (A and B) Absence of ΔF in WT and the C275A mutant. (A) Representative VCF traces of oocytes expressing ASIC1a WT, labeled with Alexa Fluor 488. (B) Representative VCF trace of the mutant C275A lacking the unique free cysteine of the extracellular domain, labeled with Alexa Fluor 488. The total fluorescence amplitude F was in WT and the C275A mutant more than fivefold smaller than in mutants showing measurable ΔF. The ΔF/F at pH 6.0 was 0.61 ± 0.07% in WT and 0.83 ± 0.11% in C275A (n = 4). These values appear greater than the corresponding ΔF values are, because the ΔF were normalized to a more than five times smaller total fluorescence amplitude F than in the other mutants. (C and D), Controls for intrinsic pH dependence of fluorophores. The figure illustrates the controls made (see also Table S1). (C) An oocyte expressing E113C was kept at a conditioning pH 6.9 for 30 s to ensure complete desensitization of the ASICs before switching to the stimulation pH 6. The conditioning at pH 6.9 resulted in the absence of current (black trace) and F (red trace) upon pH 6.0 stimulation. (D) In the same oocyte, current and ΔF were measured when the conditioning pH was 7.4.

Published December 16, 2013

this protocol may be the result of unknown, electrically silent gating transitions, such as entry in a slow desensitized state that has been proposed recently (Li et al., 2012).

Kinetics of fluorescence changes during channel activation

To identify fluorophore positions associated with channel opening or desensitization, the kinetics of the ΔF onset were compared with those of current appearance and current decay, as illustrated in Fig. 4 (A and D). As a measure of the opening kinetics, the rise time of the pH 6–induced current, corresponding to the time to pass from 10 to 90% of the peak current amplitude, was determined and compared with the rise time of the ΔF onset (Fig. 4 B). The rise time of the solution change kinetics in our experimental setting was ∼300 ms for both the current and ΔF signal (see Materials and methods). Previous studies measuring ASIC opening kinetics by using very rapid solution changes determined time constants of ∼10 ms (Bässler et al., 2001; Sutherland et al., 2001). This indicates that in our whole-oocyte measurements, the opening kinetics were limited by the kinetics of the solution change. The rise time of the current signal of WT and mutant ASIC1a (Fig. 4 B, black symbols) was in the range of ∼100–300 ms (Fig. 4, B and C), thus faster than the kinetics of solution change, suggesting that some of the channels at the oocyte surface opened before they were completely reached by the pH 6.0 solution. Because of the limited temporal resolution of the experimental system it is not possible to associate particular fluorophore positions with ASIC activation. However, we observed reproducible differences in the ΔF rise time/current rise time ratio between mutants (Fig. 4 B; Materials and methods), therefore representing real differences between mutants. Fig. 4 B shows that the ΔF onset kinetics of several mutants, as for example, D78C and E235C, were much slower than those determined for the current appearance, whereas for many other mutants, the ΔF and current onset kinetics appeared to be close to each other.

To identify fluorophore positions associated with channel desensitization from the open state, the kinetics of the ΔF onset were compared with those of the current decay. Many mutants displayed ΔF kinetics that were substantially faster than open-channel desensitization. The ΔF and current kinetics were similar to each other in the palm

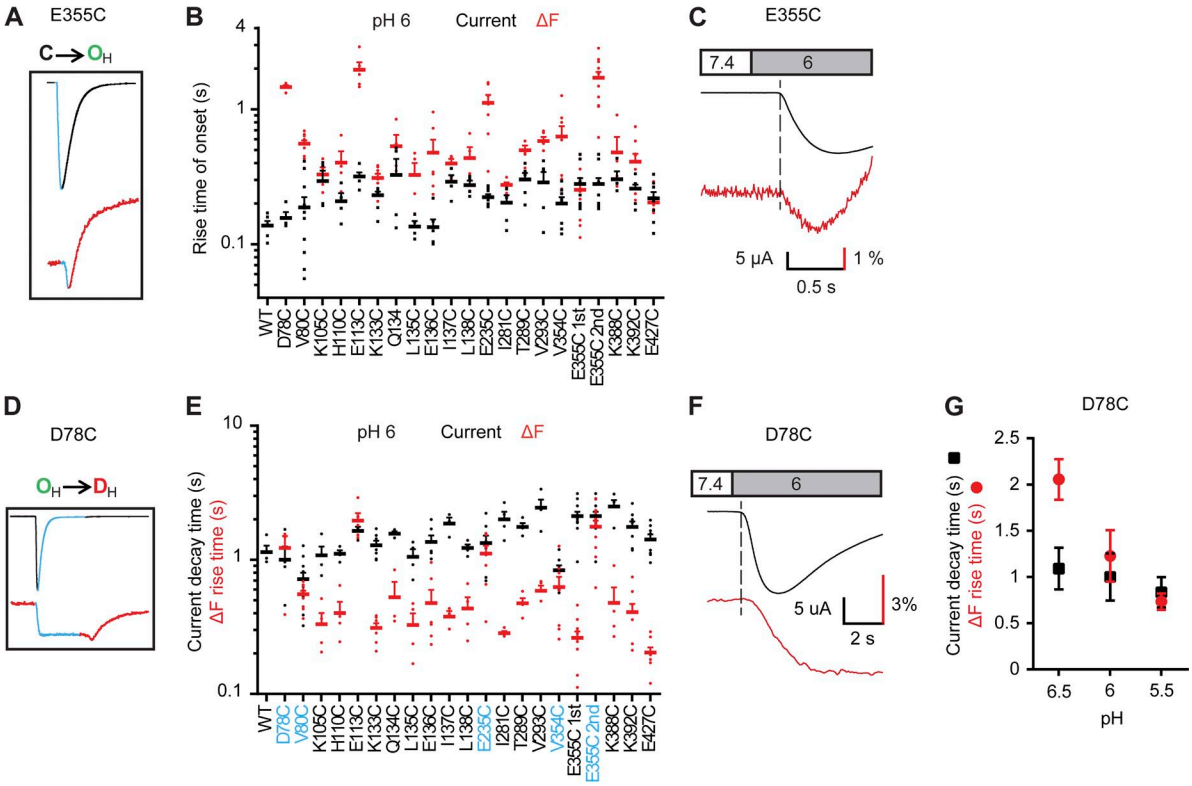

Figure 4. Kinetic analysis of the ΔF onset. (A) Schematic view illustrating in blue that in A–C, the onset kinetics of ΔF and current are compared. (B) Scatter plot summarizing ΔF onset (red) and current onset (black) rise times measured at pH 6. (C) Current and ΔF trace of a representative experiment with E355C, focusing on the rapid component of the ΔF signal. The vertical dashed line marks the beginning of the current appearance. (D) Schematic view illustrating in blue that in D–G, the ΔF onset and current decay kinetics are compared. (E) Summary graph of ΔF onset rise time (red) and current decay time (black) obtained at pH 6. Mutants whose ΔF is linked to desensitization (i.e., their ΔF rise time and current decay time are not statistically different [ANOVA and Tukey post-hoc test; $P > 0.05$], and their ratio is within the limit of 1.4-fold) are labeled in blue. (F) Current and ΔF trace of a representative experiment with D78C. The vertical dashed line marks the beginning of the current appearance. (G) Comparison of ΔF rise time (red circles) and the current decay time (black squares) of D78C at different pH. Error bars represent SEM. For B and E, $n = 4$–12; for G, $n = 4$.

Published December 16, 2013

residues D78C and V80C, the finger residue E113C, and E235C as well as the slow component of E355C, both located in the acidic pocket (Fig. 4 E). These residues are therefore associated with desensitization. Current and ΔF traces of a representative experiment with D78C illustrate a delay in the appearance of the ΔF signal (Fig. 4 F). The delay between the onset of the current and ΔF signal was in most mutants below 100 ms and only significantly increased compared with other mutants in D78C (270 ± 79 ms) and E113C (216 ± 52 ms; $n = 5$; ANOVA and Tukey post-hoc test; $P < 0.05$). The kinetics of current decay in mutants associated with desensitization were pH independent in the range of pH 6.5 to pH 5.5 (Figs. 4 G and S3). In contrast, the ΔF onset kinetics of all tested mutants were pH dependent in this pH range. As a consequence, the pH dependence curves of the ΔF onset kinetics and the current decay kinetics intersected, and values were different between ΔF and current signals at pH 6.5 for D78C and E113C (Figs. 4 G and S3). The observation that the similarity of ΔF and current kinetics does not extend over the complete pH range in these mutants suggests that open-channel desensitization is not controlled by conformational changes reported by these residues alone but involves additional conformational changes.

Alkaline shift of the ΔF pH dependence

Measurement of the pH dependence showed that fluorescence changes occurred at more alkaline pH than ionic currents, as illustrated for D78C and E355C (Fig. 5). The pH dependence midpoint of the ΔF amplitude was close to the one of SSD. Analogous to inactivation of voltage-gated Na^+ channels from the closed state, SSD is the direct transition from the closed to the desensitized state of ASICs without apparent opening (Babini et al., 2002). The alkaline shift of the ΔF relative to the current pH dependence of activation was observed in all mutants (Fig. S4 A). The pH dependence of SSD was much steeper than that of current activation (Fig. 5), consistent with previous studies (Babini et al., 2002; Krishtal, 2003). Interestingly, the steepness of the pH dependence of the ΔF amplitude was in the majority of the mutants closer to that of activation (Figs. 5 and S4 B). This illustrates the relatively shallow pH dependence of the ΔF signal in many mutants and argues against the interpretation that the observed ΔF pH dependence might simply reflect the pH dependence of SSD. The ΔF signals of most mutants could be induced at pH levels not sufficiently acidic to open the channels. Therefore, they uncover electrically silent conformational changes. Whereas some of the observed ΔF signals are associated with SSD (see below; Fig. 6), observed conformational changes with faster kinetics may prepare channel opening or desensitization.

Conformational changes associated with transitions between the closed and the desensitized state

Changes in pH known to induce SSD produced fluorescence changes with a slow onset, without inducing an ionic current (Fig. 6 A). To determine the kinetics of the functional equivalent, channels were exposed to the conditioning pH 6.9 for increasing durations before stimulation by pH 6. The decrease in current amplitude as a function of the conditioning period length was fitted to a single exponential (Fig. 6 B). The ΔF onset kinetics at pH 6.9 and the kinetics of SSD as measured by the current protocol shown in Fig. 6 B were similar to each other in the thumb mutant V354C and the finger mutant L135C (Fig. 6 C), indicating that the related conformational changes are closely linked to the closed-to-desensitized transition. In D78C, the ΔF kinetics were slightly slower than the current kinetics, and in all other mutants, the ΔF preceded the functional closed-to-desensitized transition (Fig. 6 C).

Desensitized ASICs require exposure to an alkaline pH to transit from the desensitized to the closed state before they can be activated again (Benson et al., 2002; Poirot et al., 2004). Switching the pH back to alkaline values at the end of the acidic stimulation induces recovery of the ΔF (Fig. 7 A). To determine the kinetics of the recovery of ASIC currents from desensitization, channels were first activated and completely desensitized by a test pulse to pH 6, followed by an exposure to pH 7.4 and a second test pulse to pH 6. This protocol allows measuring of the proportion of channels that

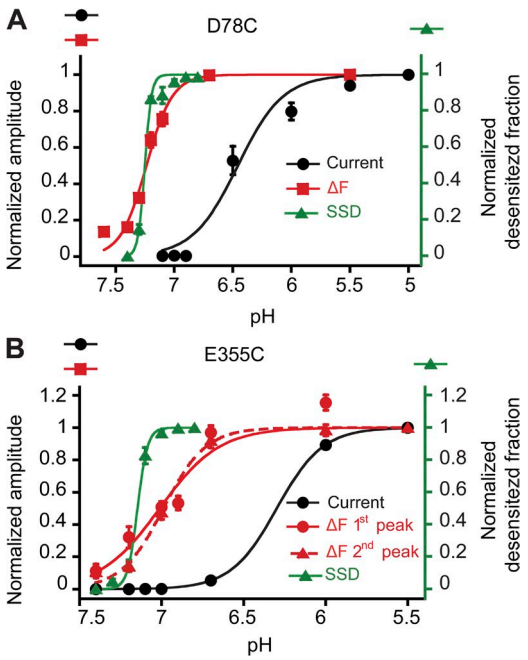

Figure 5. Fluorescence changes are detected at more alkaline pH than channel opening. Peak currents (black circles) and ΔF amplitudes (red symbols) are plotted as a function of the stimulation pH for the mutants D78C (A) and E355C (B); $n = 4–6$. The conditioning pH in these experiments was 7.8. The normalized desensitized fraction is plotted as a function of the conditioning pH to show the pH dependence of SSD (green symbols). The conditioning pH was applied during 40 s; $n = 4–5$. Error bars represent SEM.

Published December 16, 2013

had recovered from desensitization during the time spent at pH 7.4 (Fig. 7 B). The longer the interval at pH 7.4, the higher the fraction of recovered channels was. The kinetics of the ΔF and current recovery were not affected by the stimulation pH but depended on the conditioning pH to which the channels were exposed after the activation, accelerating at more alkaline pH (Fig. S5). L135C and L138C of the finger, E235C and V354C of the acidic pocket, and D78C of the lower palm domain had the same ΔF and current recovery kinetics (Fig. 7 C), indicating that they reported the transition that was limiting for preparing a subsequent opening. For several labeled residues, such as the ones of the palm-thumb loop containing the β turn, the ΔF recovery kinetics were slower than the kinetics of current recovery (Fig. 7 C and fluorescence traces in Fig. 2), revealing movements that were still ongoing when the channels had completely recovered from functional desensitization. E427C, located in the pore entry, had a fast ΔF recovery component with a time constant of ∼0.3 s in addition to the slow component (τ of ∼15 s; Figs. 7 C and 2). The time constant of current recovery was 3.1 ± 0.3 s, indicating that the movement reported by the rapid ΔF off was not sufficient for functional recovery from desensitization. E427 has previously been studied by VCF and was shown to move upon acidification with rapid kinetics (Passero et al., 2009), as in the present study.

The finger moves away from the β ball upon channel activation

The observed ΔF reflects changes in the immediate environment of the probe, such as changes in polarity or quenching upon interaction with proteins or ions. An increase in the polarity of the environment can decrease the fluorescence amplitude and shift its spectrum (Cha and Bezanilla, 1997, 1998). We tested whether the hydrophilic collisional fluorescence quencher iodide affected the fluorescence signal of the three mutants V80C, E113C and E355C in a state-dependent manner. The ratio (R) of the fluorescence intensity F in the presence of quencher/F in its absence was <1 for all three mutants, confirming the solvent accessibility of the introduced fluorophores (Fig. S6, A and B). The ratio of R at pH 7.4/R at pH 6.0 was >1 in E113C (Fig. S6 C), indicating that iodide had better access to this residue in open or desensitized than in closed channels. It is possible that the side chain of the neighboring N120 shields the

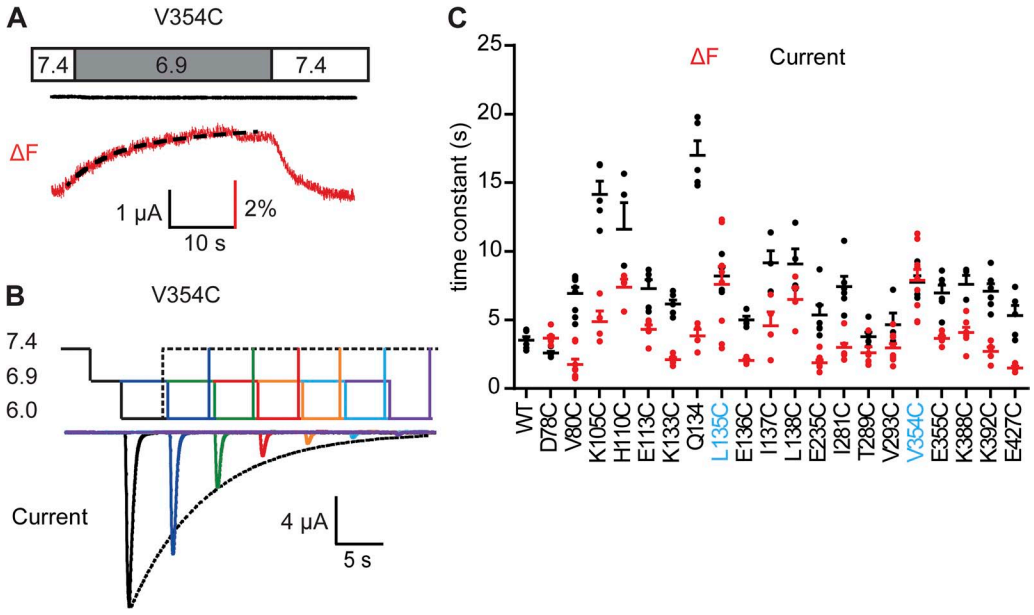

Figure 6. Fluorophores in the thumb and finger domain report movements related to SSD. (A) Representative experiment of an oocyte expressing the V354C mutant. The extracellular pH is changed as indicated from the conditioning pH 7.4 to the stimulation pH 6.9 that was not sufficiently acidic to activate the channels but generated a substantial ΔF. The onset of the ΔF was fitted to a single exponential (black dashed line). (B) Protocol applied to determine the SSD time course of ASIC1a. pH values corresponding to the different levels are indicated on the left. Channels were repeatedly activated by stimulation pH 6. Between stimulations, channels recovered during 40 s at pH 7.4. The pH 6.0 stimulation was directly preceded by incubation at conditioning pH 6.9 for a duration that increased in each round. The resulting current amplitude decrease, as a function of the incubation time at pH 6.9, was fitted to a single exponential (dotted line). (C) Time constants of the ΔF onset at stimulation pH 6.9 (red), and of the current SSD time course as determined in (B) at conditioning pH 6.9 (black), are shown for the different mutants; n = 4–10. For D78C and V80C, pH 7.0 was used instead of pH 6.9. Mutants whose ΔF is associated with SSD (i.e., their ΔF and current time constants are not statistically different [ANOVA and Tukey post-hoc test; $P > 0.05$], and their ratio is within the limit of 1.4-fold) are labeled in blue. Error bars represent SEM. All experiments were performed with fluorophore-labeled channels.

Published December 16, 2013

fluorophore placed at E113C more in the closed than in the open or inactivated conformation. In addition, protonation of the nearby H110 at more acidic pH may locally increase the I^- concentration. In the E355C mutant, the fluorophore was slightly more solvent exposed in closed than in open or desensitized channels.

Quenching groups of proteins, especially Trp residues, have been shown to contribute importantly to the ΔF (Cha and Bezanilla, 1997; Gandhi et al., 2000; Marmé et al., 2003; Pantazis and Olcese, 2012). We have tested whether Trp233, located on the β ball in close proximity of the finger, contributed to the ΔF of fluorophores placed in the α2 finger helix (Fig. 8 A). Mutation of Trp233 to Val in the mutants Q134C, L135C, and I137C suppressed the ΔF (6–13-fold reduction; Figs. 8, B and D, and S7). All tested W233V-containing double mutants were functional with the usual desensitizing current kinetics. For negative controls, we combined the W233V mutation with mutations of residues >15 Å distant from this Trp residue, E427C and H110C. The normalized ΔF amplitude was reduced by ∼40% in W233V/E427C and not changed in H110C/W233V when compared with the single mutants (Fig. 8 C). Whereas in the three double mutants with finger residues no measurable ΔF signal remained (Figs. 8 D and S7), the ΔF signal of W233V/E427C, though somewhat reduced in amplitude, preserved the same kinetics as the single E427C mutant (Fig. 8 E). This confirms that the observed ΔF with the mutants Q134C, L135C, and I137C was mainly caused by changes in quenching by Trp233. These three mutants produced positive ΔF upon acidification (Fig. 2), indicating that upon channel activation, the quenching by Trp233 decreases, thus that the finger moves away from the β ball.

Order of movements during channel activation and recovery from desensitization

Based on the kinetic analysis, we can establish the timely order of movements in the channel upon a pH change. For this comparison, the ΔF kinetics of each mutant were normalized to its current kinetics. As discussed above, the kinetics of channel opening and the related ΔF signals were limited by the kinetics of solution change. However, because differences in the ΔF onset rise time/current onset rise time ratio between mutants were statistically significant (ANOVA; $P < 0.0001$) and reproducible, and because ΔF and current kinetics were limited to the same degree by the speed of the solution change (see Materials and methods), we conclude that they represent real differences between the mutants. Residues are colored according to their normalized ΔF onset time course in Fig. 9 A. The first residues to move (orange) were several finger residues, E355C of the thumb, E427C of the pore entry, and I281C of the palm-thumb loop.

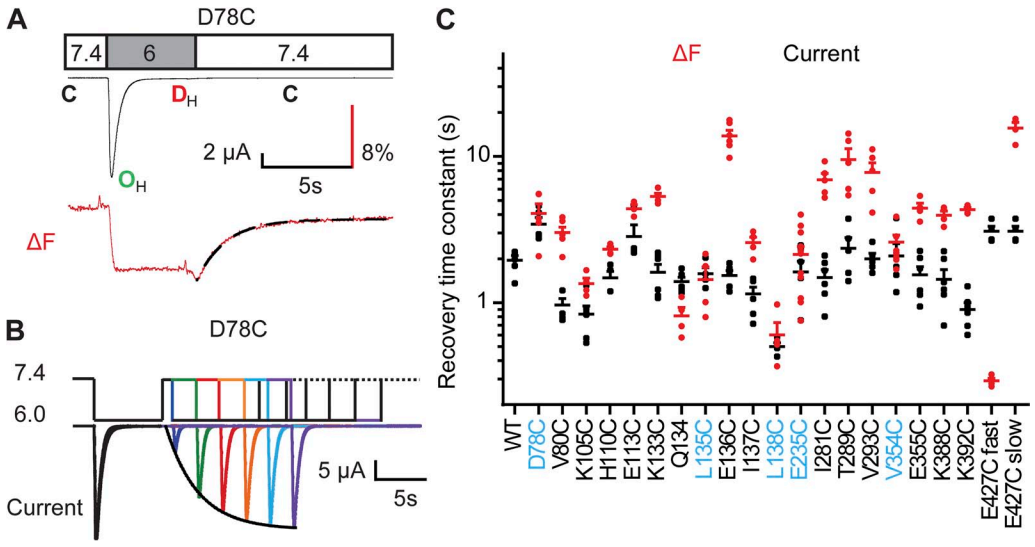

Figure 7. Recovery from desensitization is associated with conformational changes in several extracellular domains. (A) As illustrated for D78C, the fluorescence amplitude goes back to baseline when the extracellular pH is changed back to 7.4. The ΔF recovery time course was fitted to a single exponential (black dashed line). (B) To measure the kinetics of recovery from desensitization of ASIC currents, a series of paired 7-s stimulations to pH 6.0 were separated between pairs by 40 s at a conditioning pH 7.4. Within the pulse pair, the interval at pH 7.4 was kept short in the beginning and increased in each round. The amplitude of the second current amplitude normalized to that of the first stimulation was plotted as a function of the interval, and the current increase was fitted to a single exponential (dotted black line). (C) The time constants of the ΔF recovery time course (red) and the current recovery from desensitization (black) are indicated for the different mutants; $n = 3–12$. The ΔF recovery of E427C has a fast and a slow component as indicated. Mutants associated with current recovery (i.e., their ΔF and current time constants are not statistically different [ANOVA and Tukey post-hoc test; $P > 0.05$], and their ratio is within the limit of 1.4-fold) are labeled in blue. Error bars represent SEM. All experiments were performed with fluorophore-labeled channels.

Published December 16, 2013

Closely behind (yellow) followed other finger and knuckle residues and residues of the palm-thumb loop. Much slower movements (green and blue) occurred in several domains. The slowest movement, linked to desensitization, was reported by D78C of the palm (dark blue).

Upon moderate acidification inducing SSD, the order of movements is quite different from the one at pH 6.0 (Fig. 9 B). Q134C of the finger, V80C of the palm, and E427C of the pore entry moved first (red), followed by most other positions that all moved with kinetics that were faster than those of SSD. Finally, L135C and V354C moved with the same kinetics as SSD, followed only by D78C.

When the solution was switched back to pH 7.4, some finger residues were the first to report the backward movement during recovery from desensitization (Fig. 9 C), indicating that they are highly flexible. If a sequence of linked conformational changes involved several domains, the backward movement during recovery would be expected to occur in the reverse order. This was indeed observed for several residues, as for example, E235C and D78C, whose ΔF kinetics upon channel activation were very slow, whereas the recovery kinetics were faster compared with other mutants. Comparison of the order of movements during the acidification to pH 6.0 with the one during the return to pH 7.4 identified a sequence of linked conformational changes that started upon acidification with changes reported by the finger residue K133C, E427C of the pore entry, and residues of the palm-thumb loop and the knuckle. V354C and E235C of the acidic pocket and finally the palm residue D78C moved toward the end of this sequence (Fig. 9 A). The backward movement was reported first by D78C, V354C, and E235C, and toward the end of the sequence by K133C, the knuckle and palm-thumb loop residues, and the slow component of E427C.

The existence of interdependent conformational changes is further supported by the observation that in most mutants, the recovery of the fluorescence change was much slower than its onset. This difference suggests that after opening and desensitization, a bound fluorophore experienced a different structural pathway than before. The backward movement was most likely delayed by the necessity of the completion of preceding movements.

DISCUSSION

Our VCF analysis identified conformational changes in different domains that occur during channel activity. Some of these movements precede current desensitization. Fluorescence changes related to desensitization were observed in the palm, the acidic pocket, and the finger. Analysis of the order of movements suggests that the finger domain is highly flexible and moves rapidly outward upon channel activation and backward when the pH is changed back to 7.4. Residues of several domains

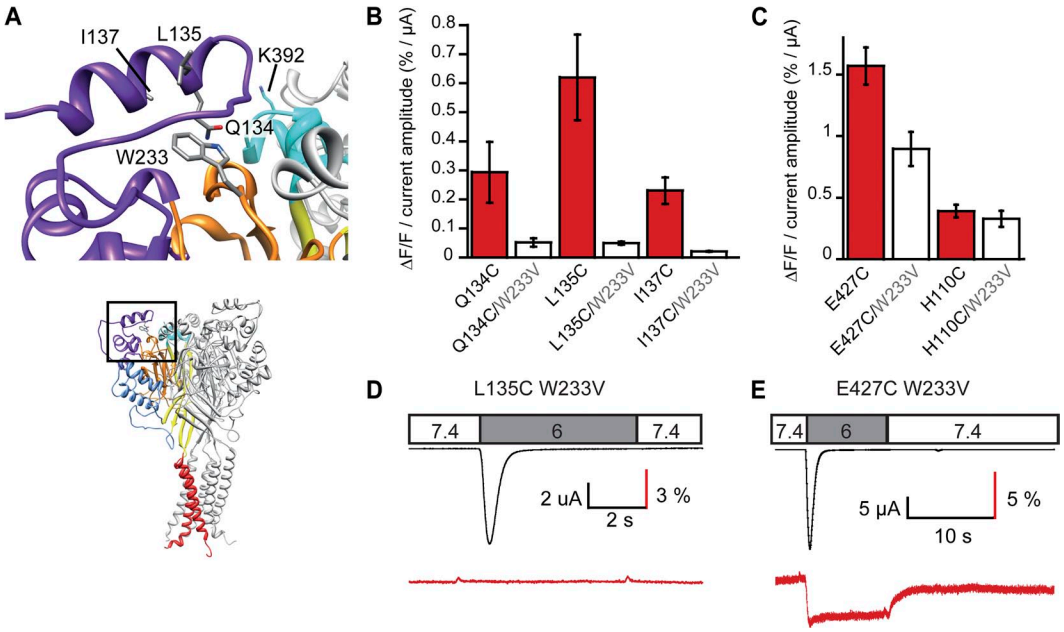

Figure 8. The finger moves away from the β ball upon channel activation. (A) View of the finger residues Q134, L135, and I137, W233 of the β ball, and K392 of the knuckle of a neighboring subunit. (B) ΔF/F normalized to the acid-induced current amplitude is indicated for the three individual finger mutants and when each of them was combined with the W233V mutation (pH 6; n = 4–10). (C) ΔF/F normalized to the acid-induced current amplitude is indicated for two control mutations at a distance of >15 Å from W233V and when each of them was combined with the W233V mutation (pH 6; n = 7–8). (D and E) Representative current and ΔF trace of the double mutant L135C/W233V and the double mutant control E427C/W233V. Error bars represent SEM.

Published December 16, 2013

are part of a sequence of conformational changes that may be linked to the entry into desensitization and recovery from it.

Conformational changes preceding desensitization

Ionic currents reflect changes in the pore. If movements of other domains occur simultaneously with ionic currents, it is expected that they are closely linked to the event in the pore. Because of the limited temporal resolution of our experiments, we cannot directly associate observed conformational changes with channel opening. However, we measured in several mutants ΔF signals that were faster than desensitization of the current, indicating that they report conformational changes either involved in channel opening or in the induction of desensitization. Such rapid conformational changes were found, for example, with residues of the finger and the knuckle. The fact that most finger mutants showed rapid changes in ΔF strongly suggests a rapid global movement of the finger during ASIC activation and/or the induction of desensitization. Differences between ΔF kinetics of finger mutants likely reflect changes in their individual microenvironment. For example, several residues oriented toward the protein body, such as E113C, L135C, and Q134C, had slower ΔF onset kinetics than residues pointing toward the

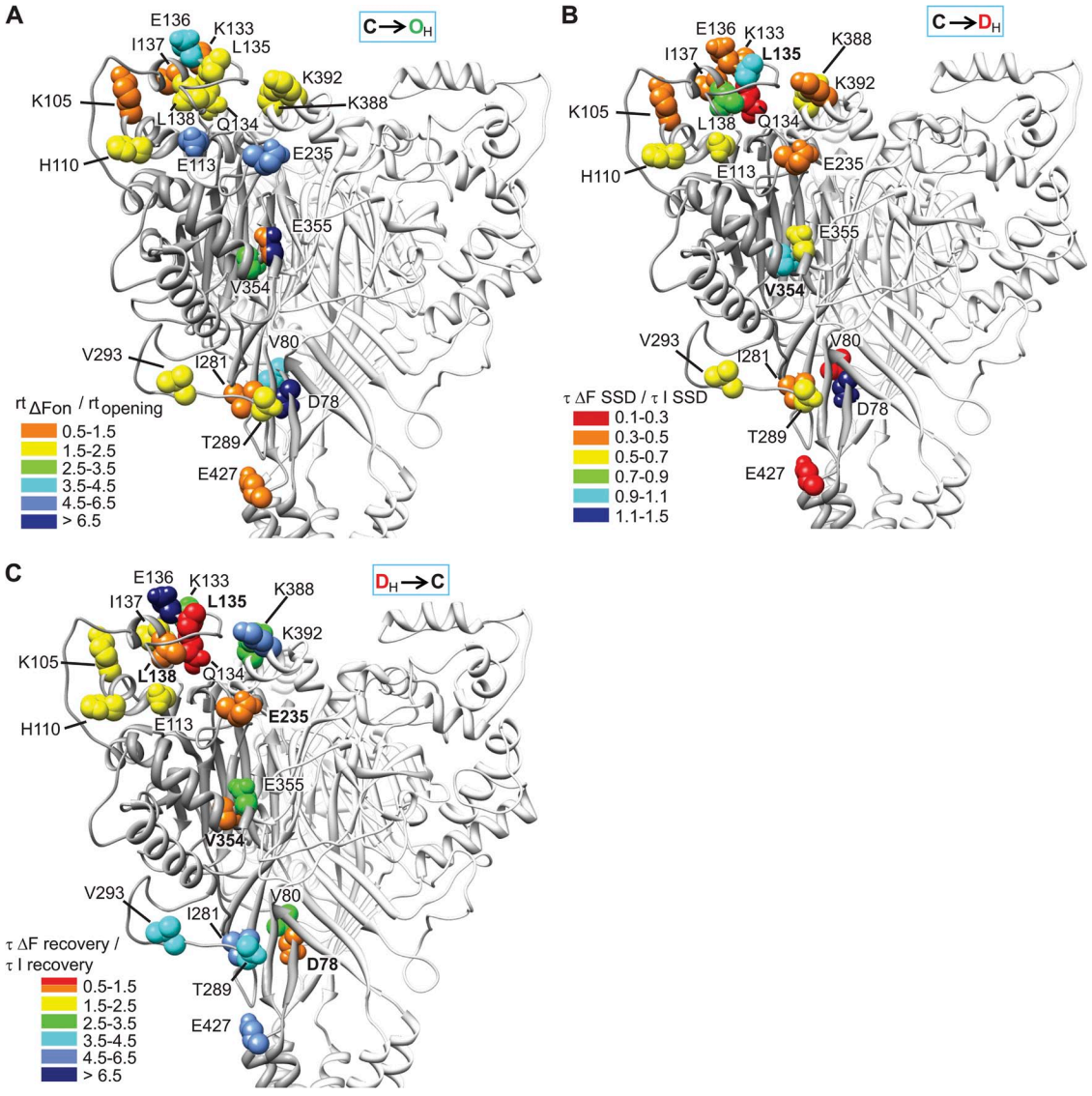

Figure 9. Rearrangements during ASIC1a gating. (A) ΔF onset. Each residue is represented in the structural model with a color corresponding to the ratio of the rise time of the ΔF onset divided by the rise time of the current onset ($rt_{\Delta Fon}/rt_{opening}$). From fast to slow, colors were orange, yellow, green, and the different shades of blue. (B) ΔF onset of SSD. Each residue is represented in the structural model with a color corresponding to the ($\tau_{\Delta F(SSD)}/\tau_{I(SSD)}$) ratio. Residues whose ΔF is associated with current SSD are labeled in bold. (C) Recovery of ΔF. Each residue is represented in the structural model with a color corresponding to the ($\tau_{\Delta Frecovery}/\tau_{Irecovery}$) ratio. Residues whose ΔF is associated with current recovery are labeled in bold.

Published December 16, 2013

protein surface. E136 was the last finger residue to report a change in the environment upon both opening and recovery, suggesting that the observed slow movement may reflect the inertia of this labeled residue. The importance of finger residues for ASIC activation has previously been highlighted with functional studies showing that mutation of some residues of this domain, and cleavage in the finger domain by proteases, profoundly affected the pH dependence of activation (Vukicevic et al., 2006; Paukert et al., 2008). Although we show that the finger moves away from the β ball, the direction of the knuckle movement remains unknown. A recent study used normal mode analysis of ASIC1 at constant pH to investigate possible conformational adaptations leading to channel opening (Yang et al., 2009). This analysis indicated the existence of collective motions between the thumb and the finger and vibrations between the knuckle and the finger, but it did not provide any evidence for a correlation of knuckle and β-ball movements.

V354C and E355C are located at the lower end of the α5 thumb helix that may have a role in the closing of the acidic pocket after protonation (Jasti et al., 2007). A first negative ΔF component in E355C was followed by a slower positive ΔF in both V354C and E355C, which showed very similar kinetics as current desensitization. After this step, E355C was less solvent exposed than in the closed conformation. Therefore, E355C undergoes a first rapid movement that is associated with channel opening or an early step of the induction of desensitization. This movement continues and eventually ends in a less exposed E355C position, consistent with the proposed closing of the acidic pocket during ASIC activation and desensitization. A rapid ΔF was also observed for I281C, a residue located in the palm at the beginning of the palm-thumb loop that contains the β turn (Fig. 1 D). Because its kinetics were similar to those of other residues in this loop and much faster than the kinetics of other palm residues, we conclude that it possibly reflects the movement of the palm-thumb loop. The fast kinetics of the ΔF onset of several pam-thumb loop residues supports a role of this loop in rapid signaling, as suggested previously on the basis of mutagenesis data (Li et al., 2009).

pH dependence of fluorescence signals

The ΔF amplitude showed a more alkaline pH dependence than the current activation in all mutants. The pH_{50} of the ΔF amplitude was for all mutants close to the pH_{50} value of SSD; however, the steepness of the ΔF amplitude pH dependence was in most mutants closer to that of channel activation. The observed shift is reminiscent of the left-shifted fluorescence relative to gating current–voltage dependence of K^+ channels (Mannuzzu et al., 1996; Cha and Bezanilla, 1997). In a multi-subunit channel requiring activation of more than one subunit for opening, some of the conformational changes are expected to occur at more alkaline pH than pore opening. In several studies with ligand-gated channels, fluorescence changes associated with channel activation showed the same concentration dependence as current activation (Chang and Weiss, 2002; Shan et al., 2011). In other studies, the concentration dependence of the ΔF associated with channel activation diverged from that of the current (Dahan et al., 2004; Pless and Lynch, 2009).

Given that our analysis indicates roles of the tested mutants in different functional transitions, it is surprising to find a very similar ΔF pH dependence in all mutants. At a pH more acidic than 7.4, conformational changes occur in all extracellular domains with similar pH dependence but different kinetics. These conformational changes are part of a general rearrangement of the ASIC protein and may be required for channel opening and desensitization. Analysis of the current and ΔF onset kinetics at higher temporal resolution might identify some of these residues as associated with opening. Alternatively, because all ΔF changes observed in our study were also found in protocols that did not lead to opening, it is possible that these conformational changes may be necessary for both opening and desensitization but may not be sufficient for opening. Additional, not yet identified mechanisms involving protonation in the pH range of activation might be required for channel opening.

Conformational changes in the palm are associated with desensitization

Movements that were likely slower than opening but substantially faster than desensitization were observed in several domains, showing that the conformational changes occurring with channel opening continue and likely prepare desensitization. We show that movements of the palm residue D78C are associated with desensitization. In addition, the ΔF recovery kinetics of D78C matched the time course of current recovery, suggesting that with the solution change to pH 7.4 the channel leaves the desensitized state when the palm undergoes a backward movement. Comparison of crystal structures indicated that the palm β sheets of the three subunits move toward the central vertical axis of the channel during desensitization (Baconguis and Gouaux, 2012). Functional evidence for such a movement has been provided by state-dependent accessibility to sulfhydryl reagents of engineered Cys residues in the palm of ASIC3 and ASIC1a (Cushman et al., 2007; Roy et al., 2013). Although the open ASIC1 structures showed a wider pore opening and a similar widening of the central vestibule relative to the desensitized structure, the other domains presented almost the same conformation in the open and desensitized structures (Baconguis and Gouaux, 2012). In contrast, our study showed evidence of conformational changes in these domains that occurred most likely after opening and before or with

desensitization. The origin of this discrepancy is currently not clear. In the crystal structures, the channel was opened by the binding of Psalmotoxin 1, and the corresponding currents showed different ion selectivity and inhibition by amiloride compared with ASIC opened by low pH. It is therefore possible that the toxin-bound open conformation does not entirely correspond to the protonated open conformation of ASIC1.

In conclusion, we show that rapid conformational changes in several domains, among them an outward movement of the finger, occur when ASIC1a is activated by protons. These conformational changes may be associated with opening or with early steps preparing desensitization. The palm-thumb loop mediates rapid events possibly linked to channel opening, whereas other parts of the palm mediate slower events that may be linked to desensitization. Our findings add a new dimension to the information on ASIC gating and will provide the basis for more detailed analyses of mechanisms that are likely shared by other ENaC/degenerin channels.

We thank Angelica Liechti, Sophie Roy, and Benoîte Bargeton for having made some of the mutants used in this study. We thank Ian Forster and Ruud Hovius for help with the construction of the VCF setup and for many discussions. We thank Omar Alijevic, Alessandro Anzelmo, Miguel van Bemmelen, Karolina Gwiazda, and Laurent Schild for their comments on the manuscript.

This work was supported by grant 130030_135542 from the Swiss National Science Foundation and by a grant from the Novartis Foundation for medical-biological research to S. Kellenberger.

The authors have no conflicting financial interests.

Edward N. Pugh Jr. served as editor.

Submitted: 25 June 2013
Accepted: 21 November 2013

REFERENCES

Babini, E., M. Paukert, H.S. Geisler, and S. Grunder. 2002. Alternative splicing and interaction with di- and polyvalent cations control the dynamic range of acid-sensing ion channel 1 (ASIC1). *J. Biol. Chem.* 277:41597–41603. http://dx.doi.org/10.1074/jbc.M205877200

Baconguis, I., and E. Gouaux. 2012. Structural plasticity and dynamic selectivity of acid-sensing ion channel-spider toxin complexes. *Nature.* 489:400–405. http://dx.doi.org/10.1038/nature11375

Bässler, E.L., T.J. Ngo-Anh, H.S. Geisler, J.P. Ruppersberg, and S. Gründer. 2001. Molecular and functional characterization of acid-sensingion channel (ASIC) 1b. *J. Biol. Chem.* 276:33782–33787. http://dx.doi.org/10.1074/jbc.M104030200

Benson, C.J., J.H. Xie, J.A. Wemmie, M.P. Price, J.M. Henss, M.J. Welsh, and P.M. Snyder. 2002. Heteromultimers of DEG/ENaC subunits form H^+-gated channels in mouse sensory neurons. *Proc. Natl. Acad. Sci. USA.* 99:2338–2343. http://dx.doi.org/10.1073/pnas.032678399

Cha, A., and F. Bezanilla. 1997. Characterizing voltage-dependent conformational changes in the Shaker K^+ channel with fluorescence. *Neuron.* 19:1127–1140. http://dx.doi.org/10.1016/S0896-6273(00)80403-1

Cha, A., and F. Bezanilla. 1998. Structural implications of fluorescence quenching in the Shaker K^+ channel. *J. Gen. Physiol.* 112:391–408. http://dx.doi.org/10.1085/jgp.112.4.391

Chang, Y.C., and D.S. Weiss. 2002. Site-specific fluorescence reveals distinct structural changes with GABA receptor activation and antagonism. *Nat. Neurosci.* 5:1163–1168. http://dx.doi.org/10.1038/nn926

Cushman, K.A., J. Marsh-Haffner, J.P. Adelman, and E.W. McCleskey. 2007. A conformation change in the extracellular domain that accompanies desensitization of acid-sensing ion channel (ASIC) 3. *J. Gen. Physiol.* 129:345–350. http://dx.doi.org/10.1085/jgp.200709757

Dahan, D.S., M.I. Dibas, E.J. Petersson, V.C. Auyeung, B. Chanda, F. Bezanilla, D.A. Dougherty, and H.A. Lester. 2004. A fluorophore attached to nicotinic acetylcholine receptor beta M2 detects productive binding of agonist to the alpha delta site. *Proc. Natl. Acad. Sci. USA.* 101:10195–10200. http://dx.doi.org/10.1073/pnas.0301885101

Dawson, R.J., J. Benz, P. Stohler, T. Tetaz, C. Joseph, S. Huber, G. Schmid, D. Hügin, P. Pflimlin, G. Trube, et al. 2012. Structure of the acid-sensing ion channel 1 in complex with the gating modifier Psalmotoxin 1. *Nat Commun.* 3:936. http://dx.doi.org/10.1038/ncomms1917

Gandhi, C.S., E. Loots, and E.Y. Isacoff. 2000. Reconstructing voltage sensor-pore interaction from a fluorescence scan of a voltage-gated K^+ channel. *Neuron.* 27:585–595. http://dx.doi.org/10.1016/S0896-6273(00)00068-4

Gonzales, E.B., T. Kawate, and E. Gouaux. 2009. Pore architecture and ion sites in acid-sensing ion channels and P2X receptors. *Nature.* 460:599–604. http://dx.doi.org/10.1038/nature08218

Jasti, J., H. Furukawa, E.B. Gonzales, and E. Gouaux. 2007. Structure of acid-sensing ion channel 1 at 1.9 Å resolution and low pH. *Nature.* 449:316–323. http://dx.doi.org/10.1038/nature06163

Kellenberger, S., I. Gautschi, and L. Schild. 1999. A single point mutation in the pore region of the epithelial Na^+ channel changes ion selectivity by modifying molecular sieving. *Proc. Natl. Acad. Sci. USA.* 96:4170–4175. http://dx.doi.org/10.1073/pnas.96.7.4170

Krishtal, O. 2003. The ASICs: signaling molecules? Modulators? *Trends Neurosci.* 26:477–483. http://dx.doi.org/10.1016/S0166-2236(03)00210-8

Li, T., Y. Yang, and C.M. Canessa. 2009. Interaction of the aromatics Tyr-72/Trp-288 in the interface of the extracellular and transmembrane domains is essential for proton gating of acid-sensing ion channels. *J. Biol. Chem.* 284:4689–4694. http://dx.doi.org/10.1074/jbc.M805302200

Li, T., Y. Yang, and C.M. Canessa. 2011. Outlines of the pore in open and closed conformations describe the gating mechanism of ASIC1. *Nat Commun.* 2:399. http://dx.doi.org/10.1038/ncomms1409

Li, T., Y. Yang, and C.M. Canessa. 2012. Impact of recovery from desensitization on acid-sensing ion channel-1a (ASIC1a) current and response to high frequency stimulation. *J. Biol. Chem.* 287:40680–40689. http://dx.doi.org/10.1074/jbc.M112.418400

Liechti, L.A., S. Bernèche, B. Bargeton, J. Iwaszkiewicz, S. Roy, O. Michielin, and S. Kellenberger. 2010. A combined computational and functional approach identifies new residues involved in pH-dependent gating of ASIC1a. *J. Biol. Chem.* 285:16315–16329. http://dx.doi.org/10.1074/jbc.M109.092015

Mannuzzu, L.M., M.M. Moronne, and E.Y. Isacoff. 1996. Direct physical measure of conformational rearrangement underlying potassium channel gating. *Science.* 271:213–216. http://dx.doi.org/10.1126/science.271.5246.213

Marmé, N., J.P. Knemeyer, M. Sauer, and J. Wolfrum. 2003. Inter- and intramolecular fluorescence quenching of organic dyes by tryptophan. *Bioconjug. Chem.* 14:1133–1139. http://dx.doi.org/10.1021/bc0341324

Meinild, A.K., B.A. Hirayama, E.M. Wright, and D.D. Loo. 2002. Fluorescence studies of ligand-induced conformational changes of the Na^+/glucose cotransporter. *Biochemistry.* 41:1250–1258. http://dx.doi.org/10.1021/bi011661r

Pantazis, A., and R. Olcese. 2012. Relative transmembrane segment rearrangements during BK channel activation resolved by structurally assigned fluorophore–quencher pairing. *J. Gen. Physiol.* 140:207–218. http://dx.doi.org/10.1085/jgp.201210807

Passero, C.J., S. Okumura, and M.D. Carattino. 2009. Conformational changes associated with proton-dependent gating of ASIC1a. *J. Biol. Chem.* 284:36473–36481. http://dx.doi.org/10.1074/jbc.M109.055418

Paukert, M., X. Chen, G. Polleichtner, H. Schindelin, and S. Gründer. 2008. Candidate amino acids involved in H^+ gating of acid-sensing ion channel 1a. *J. Biol. Chem.* 283:572–581. http://dx.doi.org/10.1074/jbc.M706811200

Pettersen, E.F., T.D. Goddard, C.C. Huang, G.S. Couch, D.M. Greenblatt, E.C. Meng, and T.E. Ferrin. 2004. UCSF Chimera—a visualization system for exploratory research and analysis. *J. Comput. Chem.* 25:1605–1612. http://dx.doi.org/10.1002/jcc.20084

Pless, S.A., and J.W. Lynch. 2009. Ligand-specific conformational changes in the alpha1 glycine receptor ligand-binding domain. *J. Biol. Chem.* 284:15847–15856. http://dx.doi.org/10.1074/jbc.M809343200

Poirot, O., M. Vukicevic, A. Boesch, and S. Kellenberger. 2004. Selective regulation of acid-sensing ion channel 1 by serine proteases. *J. Biol. Chem.* 279:38448–38457. http://dx.doi.org/10.1074/jbc.M407381200

Roy, S., C. Boiteux, O. Alijevic, C. Liang, S. Bernèche, and S. Kellenberger. 2013. Molecular determinants of desensitization in an ENaC/degenerin channel. *FASEB J.* In press.

Shan, Q., L. Han, and J.W. Lynch. 2011. β subunit M2-M3 loop conformational changes are uncoupled from α1 β glycine receptor channel gating: implications for human hereditary hyperekplexia. *PLoS ONE.* 6:e28105. http://dx.doi.org/10.1371/journal.pone.0028105

Sluka, K.A., O.C. Winter, and J.A. Wemmie. 2009. Acid-sensing ion channels: A new target for pain and CNS diseases. *Curr. Opin. Drug Discov. Devel.* 12:693–704.

Sutherland, S.P., C.J. Benson, J.P. Adelman, and E.W. McCleskey. 2001. Acid-sensing ion channel 3 matches the acid-gated current in cardiac ischemia-sensing neurons. *Proc. Natl. Acad. Sci. USA.* 98:711–716. http://dx.doi.org/10.1073/pnas.98.2.711

Virkki, L.V., H. Murer, and I.C. Forster. 2006. Voltage clamp fluorometric measurements on a type II Na^+-coupled P_i cotransporter: Shedding light on substrate binding order. *J. Gen. Physiol.* 127:539–555. http://dx.doi.org/10.1085/jgp.200609496

Vukicevic, M., G. Weder, A. Boillat, A. Boesch, and S. Kellenberger. 2006. Trypsin cleaves acid-sensing ion channel 1a in a domain that is critical for channel gating. *J. Biol. Chem.* 281:714–722. http://dx.doi.org/10.1074/jbc.M510472200

Xiong, Z.G., X.M. Zhu, X.P. Chu, M. Minami, J. Hey, W.L. Wei, J.F. MacDonald, J.A. Wemmie, M.P. Price, M.J. Welsh, and R.P. Simon. 2004. Neuroprotection in ischemia: blocking calcium-permeable acid-sensing ion channels. *Cell.* 118:687–698. http://dx.doi.org/10.1016/j.cell.2004.08.026

Yang, H., Y. Yu, W.G. Li, F. Yu, H. Cao, T.L. Xu, and H. Jiang. 2009. Inherent dynamics of the acid-sensing ion channel 1 correlates with the gating mechanism. *PLoS Biol.* 7:e1000151. http://dx.doi.org/10.1371/journal.pbio.1000151

Ziemann, A.E., J.E. Allen, N.S. Dahdaleh, I.I. Drebot, M.W. Coryell, A.M. Wunsch, C.M. Lynch, F.M. Faraci, M.A. Howard III, M.J. Welsh, and J.A. Wemmie. 2009. The amygdala is a chemosensor that detects carbon dioxide and acidosis to elicit fear behavior. *Cell.* 139:1012–1021. http://dx.doi.org/10.1016/j.cell.2009.10.029

Bonifacio et al., http://www.jgp.org/cgi/content/full/jgp.201311053/DC1

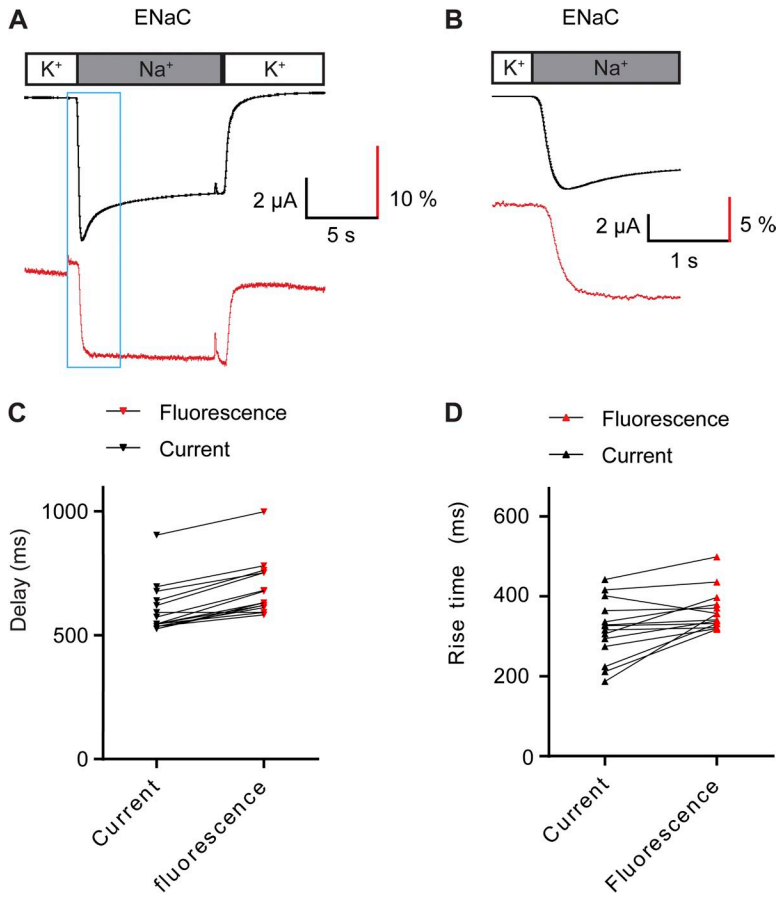

Figure S1. Kinetic parameters of the solution change. *Xenopus* oocytes were injected with cRNA encoding the α, β, and γ ENaC subunits, and ENaC was expressed as described in Kellenberger et al. (1999. *Proc. Natl. Acad. Sci. USA.* 96:4170–4175). After incubation with the plasma membrane resident pH-dependent fluorophore *N*-(fluorescein-5-thiocarbonyl)-1,2-dihexadecyl-sn-glycero-3-phosphoethanolamine, currents were induced under two-electrode voltage clamp to −40 mV by switching from an extracellular solution of pH 7.4 containing K^+ as the only monovalent cation to the normal extracellular solution containing Na^+ at pH 6.0. (A) Current and fluorescence traces from a typical experiment. (B) The same experiment is shown on an expanded time scale. (C) Individual data points of the delay from the solution switching time to the appearance of the current and ΔF signal. Solid lines connect data of the same experiment. (D) Individual data points of the rise time of the current and ΔF onset. Solid lines connect data of the same experiment; $n = 14$ from three different experimental dates.

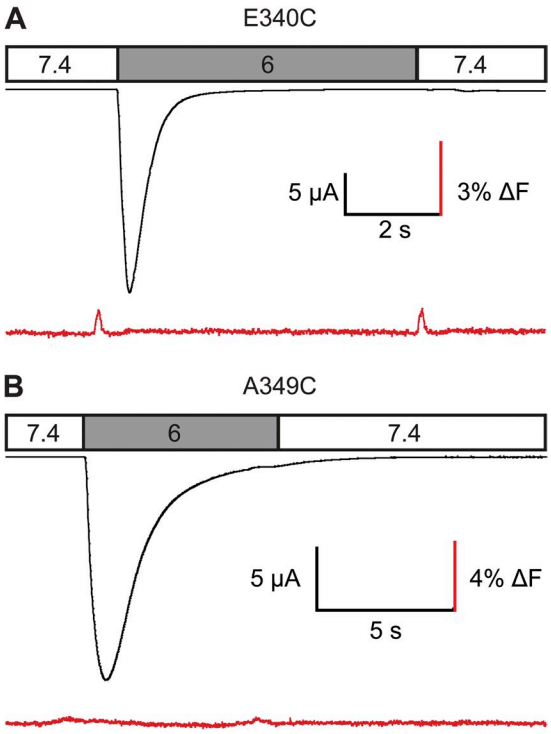

Figure S2. Mutants not producing activity-dependent ΔF signals after labeling. Current and ΔF traces of representative experiments with the two mutants, E340C (A) and A349C (B). Experiments were performed as for other mutants (see Materials and methods of main text).

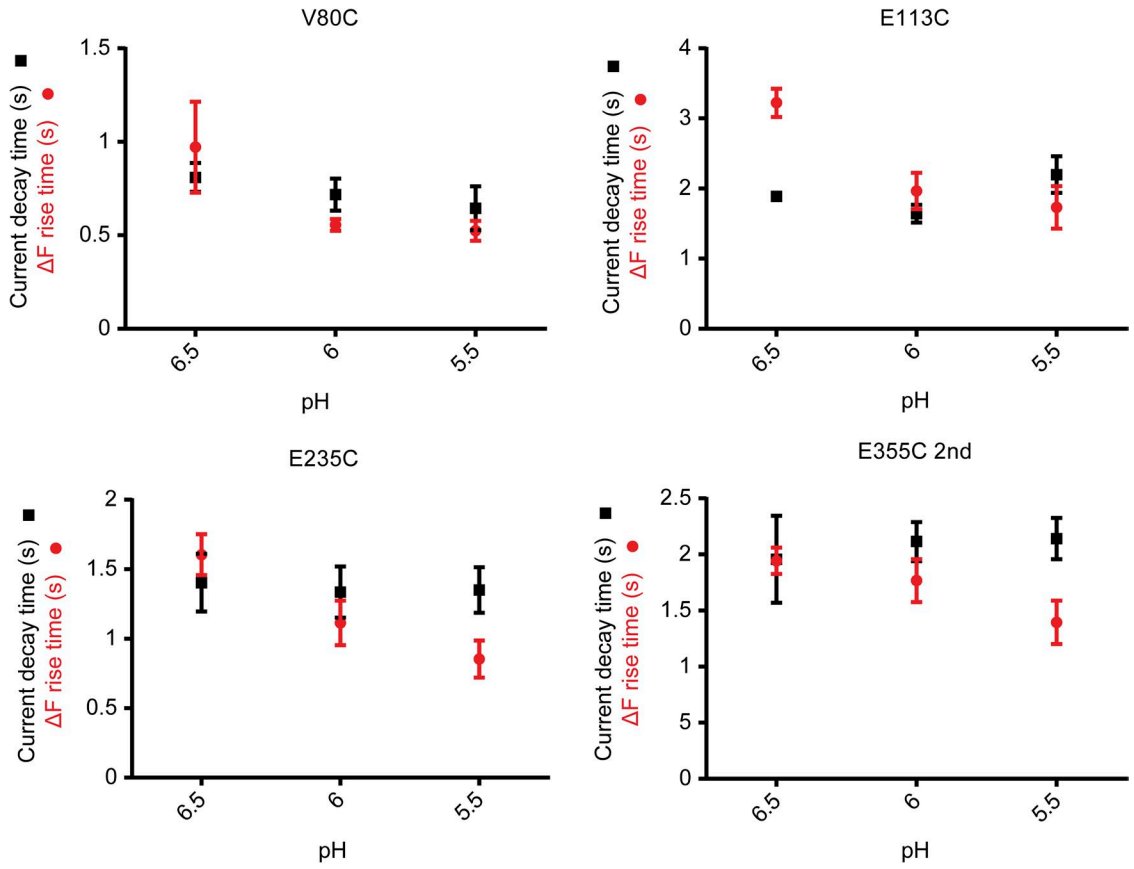

Figure S3. Current and ΔF kinetics of mutants associated with desensitization. Comparison of the rise time of the ΔF onset (red circles) and the decay time of the current (black squares) for the mutants V80C, E113C, and E235C, and the slow component of E355C; $n = 4–11$. Error bars represent SEM.

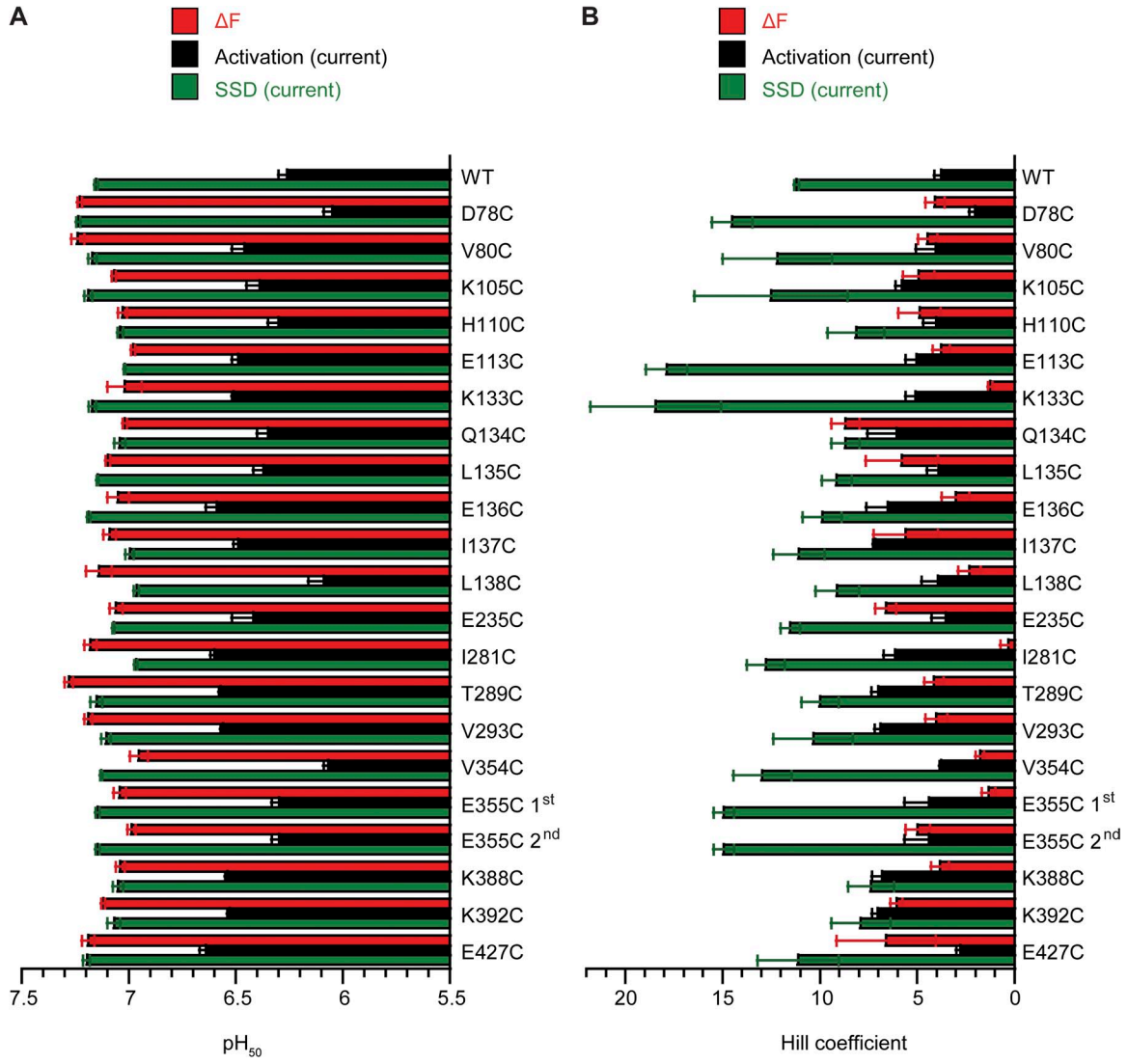

Figure S4. pH dependence of current and ΔF amplitudes. pH of half-maximal amplitude (pH_{50}; A) and Hill coefficient (B) of ΔF and current activation and SSD, obtained from analyses as shown in Fig. 5 (A and B); $n = 4–8$. The conditioning pH in activation experiments was 7.8. The exposure period to the conditioning pH in SSD experiments was 40 s, and the stimulation pH in these experiments was pH 6. Error bars represent SEM.

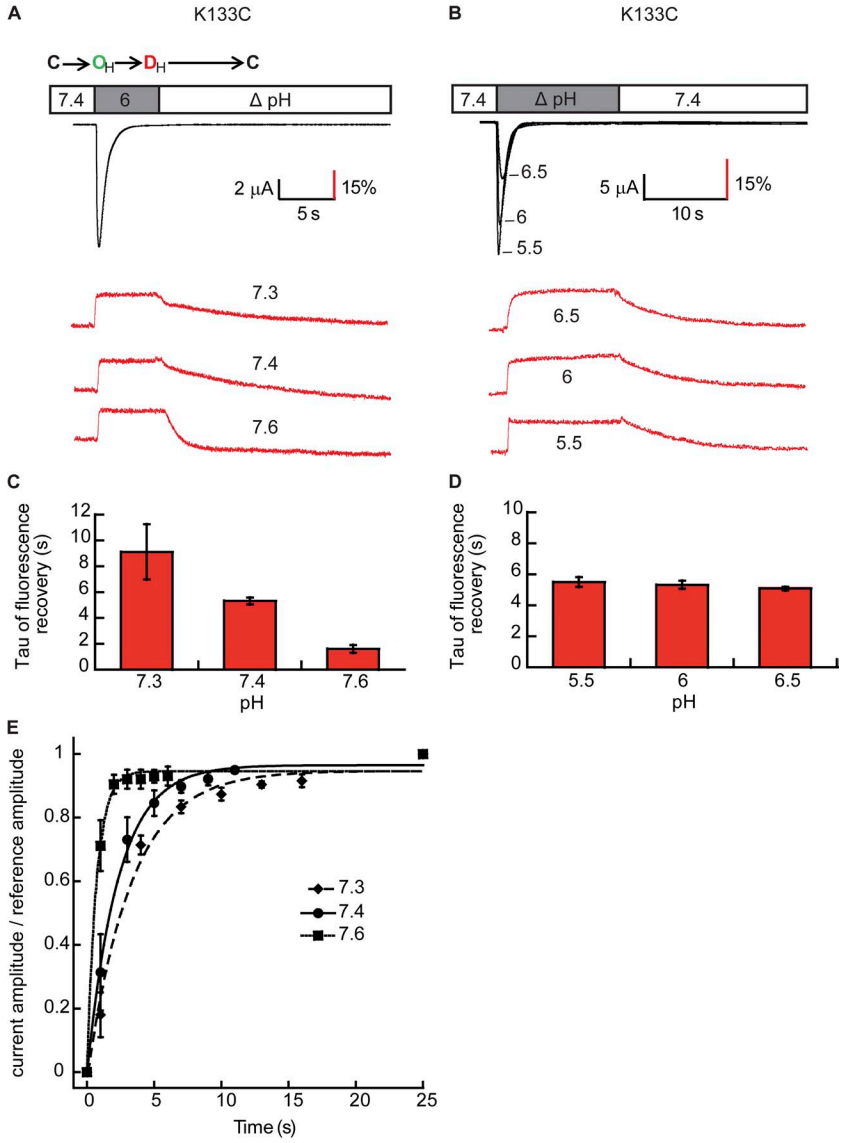

Figure S5. The kinetics of recovery depend exclusively on the conditioning pH to which the solution is returned. (A and B) Representative current and fluorescence traces from oocytes expressing K133C. In these experiments, the pH was changed to different conditioning pH values after the pH 6.0 stimulation (A), or different stimulation pH values were applied and channels were exposed to pH 7.4 after the stimulation (B). (C and D) The time constant of the ΔF recovery is shown for the conditions illustrated in A and B. (E) Time course of ASIC1a current recovery at three different conditioning pH values (7.3, 7.4, and 7.6) as a function of time. The time constants determined from exponential fits to the current recovery were 3.25 ± 0.44 s (pH 7.3), 2.32 ± 0.18 s (pH 7.4), and 0.70 ± 0.07 s (pH 7.6). The experiments were performed as described in the legend of Fig. 7; $n = 3$. Error bars represent SEM.

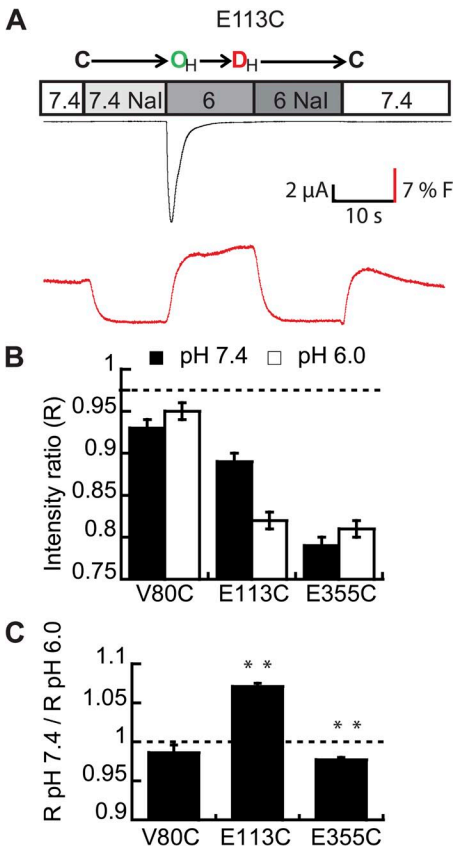

Figure S6. Quenching experiments with iodide. The fluorescence was measured in the absence/presence of iodide at both pH 7.4 and 6. Quenching solutions were prepared by replacing 100 mM Cl^- with the same concentration of I^-. (A) Current and ΔF traces from an experiment with E113C. (B) The ratio $R = F(I^-)/F(Cl^-)$ is shown at pH 6.0 (open bars) and pH 7.4 (closed bars). (C) The ratio of $R_{pH7.4}/R_{pH6.0}$ is shown for the three mutants. **, $R_{pH7.4}$ / $R_{pH6.0}$ different from 1 ($P < 0.01$); $n = 4–7$. The error bars represent SEM.

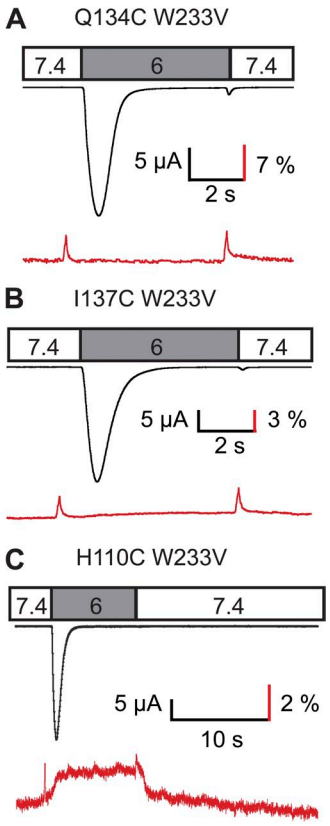

Figure S7. Current and ΔF traces of double mutants. Current and ΔF traces from representative experiments are shown for the mutants Q134C/W233V (A), I137C/W233V (B), and H110/W233V (C). The small ΔF peaks in A and B are artifacts caused by the solution change.

Table S1
Test for intrinsic pH dependence of fluorophores

Mutant	Ratio (%) $^{\Delta F}/_{F}$ desensitized-to-open/$^{\Delta F}/_{F}$ closed-to-open protocol
D78C	1.6 ± 0.6
V80C	8.1 ± 3.2
K105C[Ca]	9.0 ± 1.6
H110C[a]	3.6 ± 1.7
E113C	9.4 ± 2.2
K133C	9.7 ± 3.0
Q134C	11.4 ± 2.5
L135C[Ca]	11.4 ± 3.5
E136C	23.7 ± 2.2
I137C[a]	3.3 ± 1.0
L138C[a]	14.8 ± 2.6
E235C	9.3 ± 1.8
I281C[Ca]	5.3 ± 1.7
T289C[C]	20.1 ± 3.9
V293C[Ca]	6.6 ± 0.5
V354C[C]	15.8 ± 1.5
E355C	7.9 ± 2.7
K388C[Ca]	15.4 ± 3.4
K392C[Ca]	1.2 ± 0.7
E427C	9.6 ± 3.1

The ratio of the ΔF/F of the desensitized-to-open protocol (i.e., pH 6.9 to 6)/ΔF/F of the closed-to-open protocol (pH 7.4 to pH 6) is shown as a percentage (n = 4 ± SEM). For most mutants, this ratio was measured using the two fluorophores Alexa Fluor 488 and CF488. The fluorophore yielding the lower ratio was subsequently used for the experiments and its ratio (as a percentage) is indicated in this table. Mutants labeled by CF488 are marked with C. Alexa Fluor 488 was used for all the remaining mutants.

[a]In these mutants, the desensitized-to-open protocol was carried out at pH 6.8 and 6.